Structural characterization of protein–DNA complexes using small angle X-ray scattering (SAXS) with contrast variation

Stephanie Hutin, Audrey Guillotin, Chloe Zubieta, Mark A. Tully

▶ **To cite this version:**

Stephanie Hutin, Audrey Guillotin, Chloe Zubieta, Mark A. Tully. Structural characterization of protein–DNA complexes using small angle X-ray scattering (SAXS) with contrast variation. Methods in Enzymology, 680, Elsevier, pp.163-194, 2023, 0076-6879. 10.1016/bs.mie.2022.1008.1021 . hal-03813271

HAL Id: hal-03813271
https://hal.science/hal-03813271

Submitted on 17 Oct 2022

HAL is a multi-disciplinary open access archive for the deposit and dissemination of scientific research documents, whether they are published or not. The documents may come from teaching and research institutions in France or abroad, or from public or private research centers.

L'archive ouverte pluridisciplinaire **HAL**, est destinée au dépôt et à la diffusion de documents scientifiques de niveau recherche, publiés ou non, émanant des établissements d'enseignement et de recherche français ou étrangers, des laboratoires publics ou privés.

Structural characterization of protein-DNA complexes using Small Angle X-ray Scattering (SAXS) with contrast variation

Stephanie Hutin [a], Audrey Guillotin[a], Chloe Zubieta [a*] and Mark Tully [b*]

[a] Laboratoire Physiologie Cellulaire et Végétale, Univ. Grenoble Alpes, CNRS, CEA, INRAE, IRIG-DBSCI-LPCV, 17 Avenue des Martyrs, 38054, Grenoble, France. e-mail chloe.zubieta@cea.fr

[b] European Synchrotron Radiation Facility, Structural Biology Group, 71 Avenue des Martyrs, 38000 Grenoble, France. e-mail mark.tully@esrf.fr

*corresponding authors

Abstract

Molecular and atomic level characterization of transcription factor (TF)-DNA complexes is critical for understanding DNA-binding specificity and potentially structural changes that may occur in protein and/or DNA upon complex formation. Often TFs are large, multi-domain proteins or contain disordered regions which contribute to DNA recognition and/or binding affinity but are difficult to structurally characterize due to their high molecular weight and intrinsic flexibility. This results in challenges to obtaining high resolution structural information using NMR spectroscopy due to the relatively large size of the protein-DNA complexes of interest or macromolecular crystallography due to the difficulty in obtaining crystals of flexible proteins. Small angle X-ray scattering (SAXS) offers a complementary method to NMR and X-ray crystallography, allowing the low-resolution structural characterization of protein, DNA and protein-DNA complexes in solution over a greater size range and irrespective of interdomain flexibility or disordered regions. One important caveat to SAXS data interpretation, however, has been the inability to distinguish between scattering coming from the protein versus DNA component of the

complex of interest. Here, we present a protocol using contrast variation via increasing sucrose concentrations to distinguish between protein and DNA using the model protein bovine serum albumin (BSA) and DNA and the LUX ARRYTHMO transcription factor-DNA complex. Examination of the scattering curves of the components individually and in combination with contrast variation allows the differentiation of protein and DNA density in the derived models. This protocol is designed for use on high flux SAXS beamlines with temperature-controlled sample storage and sample exposure units.

Keywords: small angle X-ray scattering, transcription factors, protein-DNA complexes, contrast variation

1. Introduction

Transcription factors (TFs) are a class of DNA-binding proteins that recognize short sequences of DNA and bind these motifs with high specificity in the crowded nuclear environment, allowing the activation or repression of target genes. Due to their central role in regulating gene expression, the structure of DNA-binding domains of TFs have been studied for decades in order to decipher their sequence specific binding (Pabo, Carl O. 1992; Wolberger 1993; Wolberger 2021). *In vitro* studies of many TF and TF-DNA complexes using macromolecular crystallography and NMR spectroscopy have revealed that both protein and DNA often undergo structural changes upon complex formation (Andrabi et al. 2014; Chu et al. 2014; Poddar et al. 2018). These structural changes contribute to the affinity and specificity of complex formation and likely play important roles *in vivo* by altering local chromatin structure or allowing for the recruitment of ternary factors by the TF. However, many TFs and TF-DNA complexes do not crystallize and are too large for NMR studies, limiting our ability to structurally investigate these interactions. New algorithms allow for the structural predictions of different TFs, but often exhibit low probability for regions of high flexibility or high intrinsic disorder that may be important for DNA binding affinity and/or specificity (Jumper et al. 2021). Predicting DNA structure and structural changes upon TF binding are even more limited and often neglected, although these changes are often required in the context of chromatin for TF target gene activation or repression. One important tool for structural characterization of TF, DNA and TF-DNA complexes is small angle X-ray scattering (SAXS). In SAXS experiments, X-rays are scattered by the electrons in solution and data are measurable at small angles close to the direct beam (generally less than 5°). While SAXS is limited to resolutions in the low nanometer range, important information as to size, flexibility and shape of macromolecules is obtainable, providing an electron density envelope that may be fit with high resolution data obtained experimentally from crystallography or NMR experiments or predicted models.

SAXS has been used to structurally characterize a multitude of soft matter and biological macromolecules in aqueous solutions including polymers, detergents, lipids, colloids, intrinsically disordered proteins and nucleic acids (Ballauff 2001; Chu and Hsiao 2001; Bolze et al. 2003; Kikhney and Svergun 2015; Dwivedi and Lepkova 2017; Kiselev and Lombardo 2017). The versatility of the technique allows measurements using an extensive variety of conditions spanning a broad range of macromolecular species as well as different buffer pHs, ionic strength and measurement temperatures. SAXS has been extensively applied to different protein and protein complexes and may be used in conjunction with high resolution techniques to obtain biologically relevant models of large macromolecular species inaccessible using a single structural technique (Putnam et al. 2007; Classen et al. 2013; Rambo and Tainer 2013a).

For determining the structure of different TF-DNA complexes using SAXS, X-ray scattering measurements of each partner individually and in complex can be performed. X-rays are scattered by the particles in solution and data is displayed as the intensity of the scattered X-rays as a function of the scattering vector, q, in which

$$q=\frac{4\pi}{\lambda}\sin\theta$$

where λ is the wavelength and θ is half the scattering angle. The intensity of the measured signal depends on the square of the electron density difference between the particles in solution (ρ) and the solvent (ρ_{sol}). The scattering vector, q, is dependent on the size and shape of the particles in solution (form factor) and possible long-range interactions between particles (structure factor). Scattering data allows the direct calculation of a radius of gyration, *Rg*, an excluded particle volume, the molecular weight and the maximum dimension, D_{max}. Detailed protocols for analyzing SAXS data are available for different biological macromolecules including folded and disordered proteins, RNA and DNA(Putnam et al. 2007; Rambo and Tainer 2010a; Rambo and Tainer 2010b; Burke and Butcher 2012; Rambo and Tainer 2013b; Kikhney and Svergun 2015; Chen and Pollack 2016). As SAXS measurements are based on a detectable scattering difference between the species in solution and the surrounding solvent, for dilute species and weak scatterers,

high intensity synchrotron sources are required to obtain sufficient signal to noise to differentiate between the species of interest and the surrounding solvent. To obtain a good data set it is essential that the samples are monodisperse. On many biological synchrotron based SAXS beamline, inline chromatographic techniques are available to maximize the purity of the sample by reducing the time between the purification and SAXS measurement for reducing potential aggregation (Round et al. 2013; Brennich et al. 2016; Hutin et al. 2016; Tully et al. 2021). In addition, it must be noted that SAXS is not an atomic resolution technique and will only provide structural information in the low nanometer range (generally $\sim 0.1° < 2\theta < 5°$ which corresponds to $0.01 < q < 0.35$ Å^{-1}). Large conformational changes, however, are measurable by SAXS and have been shown for many different proteins and protein complexes (Hura et al. 2013; Brosey and Tainer 2019).

One drawback of SAXS measurements of TF-DNA complexes, and protein nucleic acid complexes in general, is the inability to distinguish between scattering from protein versus DNA in the complex, as SAXS measures differences in the scattering from the particles in solution versus the solvent or buffer without particles. In order to address this limitation, contrast variation may be used in which the electron density coming from one species in the complex is "matched out," resulting in measured scattering from only one component of the TF-DNA complex (Chen et al. 2017). Contrast variation uses different additives such as sucrose (Dingenouts and Ballauff 1993; Kidd and Proctor 2001; Ballauff 2001; Kiselev et al. 2001; Bolze et al. 2003; Garcia-Diez et al. 2016), glycerol (Bolze et al. 1996; Hickl et al. 1996) and salt (Fernandez et al. 2008; Naruse et al. 2009) to alter the electron density of the solvent, effectively "matching" it to the electron density of one component of the complex. For example, once the electron density of the solvent is close to the electron density of protein in the TF-DNA complex, only scattering from the high electron density DNA is observed in the SAXS curve. By systematically altering the electron density of the solvent the internal electron density profile of different macromolecular systems can be probed (Gabel et al. 2019). While protocols for studying lipid-protein complexes using contrast variation and small angle scattering (neutron and X-ray) have been published, to

the best of our knowledge there are no detailed protocols for contrast variation for protein-DNA complexes.

Here, we use bovine serum albumin (BSA) and LUX ARRHYTHMO (LUX) as a model protein to demonstrate contrast variation and solvent matching. By systematically varying the concentration of sucrose, the scattering of BSA alone and from a mixture of BSA and DNA, the BSA becomes largely undetectable. In the BSA and DNA mixture, however, the scattering from DNA is still detectable in the high sucrose buffer, allowing structural analysis of the DNA component alone. Comparing the scattering of DNA in buffer, buffer with added sucrose and contrast matched BSA/DNA mixture demonstrates that the DNA retains the same size and shape based on R_g, volume and D_{max} calculations, standard structural parameters obtained from any SAXS experiment. Examination of a TF-DNA complex using the same experimental pipeline shows similar results, with successful contrast matching of the TF. We discuss the application of this protocol to different TF-DNA complexes, the various strengths and drawbacks of the technique, the optimization steps required and the versatility of experimental conditions that may be sampled including the use of different additives for contrast matching and the facile study of TF-DNA complexes at different temperatures in the same experiment.

2.1 Protein sample and buffer preparation

SAXS experiments require milligram amounts of material for measurement. While high intensity synchrotron sources, modern pixel detectors and improved optics have allowed the study of smaller volumes of sample at lower concentration, radiation damage to the sample must be considered and any measurement will still require 50-100 µl of sample at a minimum of 0.5 mg/ml. Higher concentrations of sample allow data collection with better signal to noise at higher resolution and more reliable models. Multiple measurements are generally required for each sample for individual components in the matching purification buffer, the TF-DNA complex of interest in its matching purification buffer, and the same measurements carried out in high sucrose buffers. Due to these

sample requirements, recombinant expression of the TF of interest is recommended. DNA may be commercially synthesized or PCR amplified keeping in mind the quantities and purity required for SAXS measurements.

Below is a protocol for purification of the plant-specific TF, LUX ARRHYTHMO (LUX). LUX is a core component of the circadian clock and, in conjunction with its partners EARLY FLOWERING 3 and 4 (ELF3 and ELF4), serves as a night time regulator of temperature dependent elongation growth(Nusinow et al. 2011; Ezer et al. 2017; Silva et al. 2020). LUX contains 323 amino acids with a single ~50 amino acid MYB DNA-binding domain with largely disordered regions adjacent to the MYB domain (Figure 1). We use LUX alone and in complex with DNA as a model system to illustrate protein expression, complex formation and purification workflows. This protocol includes recombinant expression of the 6xHis-tagged LUX protein, DNA oligomer annealing, complex formation and FPLC purification. It should be noted that all these steps must be performed before any attempt at measuring SAXS data. The buffers used and conditions of complex formation are variable and specific to the TF and TF-DNA complex of interest and must be adapted accordingly.

BEFORE YOU BEGIN

Timing: 3h

1. All buffers and reagents for protein expression and purification should be freshly prepared, particularly buffers including protease inhibitors and reducing agents. Buffers should be kept at 4° C or on ice.

2. Buffers and solutions
    1. Lysis buffer: 200 mM N-cyclohexyl-3-aminopropanesulfonic acid (CAPS), pH 10.5, 500 mM NaCl, 1 mM Tris(2-carboxyethyl)phosphine (TCEP), and protease inhibitors (Roche)
    2. High salt buffer: 200 mM CAPS, pH 10.5, 500 mM NaCl, 1 mM Tris(2-carboxyethyl)phosphine (TCEP), and protease inhibitors

3. Elution buffer : 200 mM CAPS, pH 10.5, 500 mM NaCl, 300 mM imidazole,1 mM TCEP
4. Dialysis buffer : 200 mM CAPS, pH 10.5, 500 mM NaCl,1 mM TCEP
5. Size exclusion chromatography (SEC) buffer: 50 mM CAPS, pH 9.7, 100 mM NaCl, and 1 mM TCEP
6. Laemmli buffer
7. DNA binding buffer:10 mM Tris, pH 7.0, 50 mM NaCl, 1 mM $MgCl_2$, 1 mM TCEP, 3 % glycerol, 28 ng/µL herring sperm DNA, 20 µg/mL BSA, 2.5 % 3-cholamidopropyl dimethylammonio 1-propanesulfonate:CHAPS), 1.25 mM spermidine.
8. 10 x tris-borate-EDTA (TBE) buffer (10x TBE 1 liter stock solution): Dissolve 108 g Tris and 55 g Boric acid in 900 mL distilled water, add 40 mL 0.5 M Na_2EDTA (pH 8.0) (alternatively use 9.3 g Na_2EDTA), adjust volume to 1 liter.

KEY RESOURCES TABLE

REAGENT or RESOURCE	**SOURCE**	**IDENTIFIER**
Bacterial Strains		
RosettaTM 2(DE3)pLysS Competent Cells	Sigma	71403-4
Chemicals, Peptides, and Recombinant Proteins		
Kanamycine sulfate	Roth	T832.2
Chloramphenicol	Sigma	C0378
IPTG	Roth	CN08.4 300
Bovine Serum Albumin	Sigma	A7638-5G
LB-medium (Lennox), granulated	Roth	6669.4
N-cyclohexyl-3-aminopropanesulfonic acid (CAPS, CAS: 1135-40-6)	Sigma	C2632
Ni sepharose 6 fastflow	Cytiva	GE17-5318-06
NaCl	Roth	3957.1
Tris-(2-carboxyéthyl)-phosphine chlorhydrate (TCEP)	Roth	HN95.4 280
cOmplete(TM), EDTA-free Protease Inhibitors Sigma	Sigma	5056489001

Imidazole CAS 288-32-4	Sigma	I0125
TEV 1 mg/mL	in-house production	
InstantBlue Coomassie Protein Stain or similar	Sigma Aldrich	
Tris base	Sigma Aldrich	93350
Precision Plus Protein dual color standard	Bio-Rad	1610374
$MgCl_2$ CAS 77786-30-3	Sigma	M8266
Glycerol (CAS 56-81-1)	Carlo Erba	453752
herring sperm DNA	ThermoFisher	15634017
3-cholamidopropyl dimethylammonio 1-propanesulfonate (CHAPS)	ThermoFisher	B21927.14
Boric acid	Duchefa	B0503
Na_2EDTA (CAS 6381-92-6)	Euromedex	EU0007
Acrylamide	ThermoFisher	330221000
TEMED (tetramethylethylenediamine)	ThermoFisher	17919
APS (ammonium persulfate)	ThermoFisher	17874
Sucrose	ThermoFisher	J21931.36
Oligonucleotides		
DNA FW (5′-CCAAGATTCGAAGGCCG 3′) (HPLC purified, 1 µmol) for SAXS	Eurofins genomics (hplc purified)	
DNA REV (5′-CGGCCTTCGAATCTTGG 3′) (HPLC purified, 1 µmol) for SAXS	Eurofins genomics (hplc purified)	
DNA EMSA FOR (5′- Cy5-ATGATGTCTTCTCAAGATTCGATAAAAATGGTGTTG-3′	Eurofins genomics (hplc purified)	
DNA EMSA REV (CAACACACCATTTTTATCGAATCTTGAGAAGACATCAT-3′)	Eurofins genomics (hplc purified)	
Recombinant DNA		
LUX (LUX FL; The Arabidopsis Information Resource [TAIR] At3g46640.1) in pESPRIT002 expression vector		

MATERIALS AND EQUIPMENT

- Beckman Coulter Avanti J-26 XP centrifuge with the rotor JLA 8.1000 or similar
- Beckman Coulter Avanti J-26 XP centrifuge with the rotor JA-25.25 or similar

- Sonicator (Branson Sonifer 250) or similar
- Ice bucket
- spin concentrator (Amicon Ultra 4, Ultracel -10 k, Ref : UFC801096)
- Superdex 200 Increase 10/300 GL (cytiva, 28990944)
- AktaPure or Biorad fplc protein purification system or similar
- SDS gel (home-made or Mini-PROTEAN TGX, Stain-free Gels, 12 %, Ref: 4568046)
- SDS running chambers
- ChemiDoc (ThermoFisher) or similar
- 1.5 mL reaction tubes
- 0.2 mL PCR strips
- Pipettes and pipette tips

STEP-BY-STEP METHOD DETAILS

The expression and purification of the TF of interest should follow established protocols if available and conditions may vary considerably from the protocol presented here. Protocol optimization by the user may be required.

Protein expression and purification:

Timing: 3 days

3. Protein expression in *E. coli* BL21 (DE3) Rosetta cells

    1. Transform BL21 (DE3) Rosetta cells with the pESPRIT2 vector containing the full-length LUX cDNA and plate onto an agar plate supplemented with 50 μg/mL kanamycin.
    2. Incubate overnight at 37° C.
    3. Select a single colony and inoculate 100 mL LB supplemented with chloramphenicol (100 μg/mL) and kanamycin (50 μg/mL). Grow the culture over night at 37C.

4. Inoculate 1L LB supplemented with chloramphenicol (100 μg/mL) and kanamycin (50 μg/mL) with 10-15 mL of overnight culture and grow at 37˚ C until an A_{600} of 1.0 is reached.
5. Reduce the temperature to 18˚ C and add 1 mM IPTG.
6. Grow cells overnight at 18˚ C.
7. The next day, spin the cells at 4500 x g for 20 min. to pellet.
8. Resuspend the bacterial pellets in 25 mL lysis buffer per liter of expression and lyse by sonication in lysis buffer.
9. Sonicate the sample in an ice bucket with an ice water mixture (12 min, 50 %, power setting 8).
10. Spin the lysate at 45000 x g for 30 min.
11. Collect the supernatant.
12. Load the supernatant onto a 1.5 mL nickel affinity column pre-equilibrated with lysis buffer
13. Wash with 25 CV lysis buffer without protease inhibitors.
14. Wash with 50 CV high salt buffer (lysis buffer with 1 M NaCl).
15. Elute the protein in 500 μL steps in elution buffer.
16. Run an SDS gel in Laemmli buffer and stain it with Coomassie or Instant Blue to visualise the eluted protein.
17. Combine the fractions of interest.
18. Optional: Mix with 100 μL 1 mg/mL TEV protease to cleave the His-tag.
19. Dialyse the elution overnight in dialysis buffer.
20. Apply the protein to a 1.5 mL Ni-column pre-equilibrated with dialysis buffer (the same column from step 12 may be used if the resin has been washed of elution buffer and equilibrated in dialysis buffer) and wash with 3 mL lysis buffer without protease inhibitor and collect the flow through and the wash.
21. Concentrate the protein to ~10 mg/mL using a spin concentrator (the protein concentration may vary depending on the TF of interest. Generally, the higher the protein concentration the better the SAXS signal, however care must be taken to avoid aggregation and/or precipitation of the sample).

22. Prepare the FPLC system and equilibrate a Superdex 200 column in SEC-buffer.
23. Inject LUX onto the column and collect 1 mL fractions using a fraction collector.
24. Run an SDS gel of the peak fractions in Laemmli buffer and stain it with Coomassie or Instant Blue to assess the purity of the sample. Samples should be greater than 95 % pure.
25. Select and pool the fractions of interest and concentrate to ~ 10 mg/mL.

Pause Point: The protein can be stored at 4° C overnight or flash frozen and stored at -80° C over several months

4. Anneal the DNA oligomers to create a double stranded DNA:

    1. Resuspend the oligomers at a concentration of 1 mmol in nuclease-free water.
    2. Mix equivalent amounts of the forward and reverse oligomers in an Eppendorf tube.
    3. Close the tube. Parafilm may be used to ensure proper sealing.
    4. Boil 500 mL water in a 1 L glass beaker in the microwave and transfer it to a heating plate set for 95° C.
    5. Place the sample into an Eppendorf tube floater in the hot water.
    6. Heat the DNA for 5 min at 95° C.
    7. Place the beaker without taking the sample out onto a heat resistant benchtop area.
    8. Let the water reach room temperature.

Pause Point: The DNA can be stored at -20° C over several months.

We recommend verifying the DNA-binding activity of the TF of interest using electrophoretic mobility shift assays (EMSAs). This will allow testing different binding buffer conditions (salt concentrations, pH, etc.) to ensure stable complex formation for large scale purification of the TF-DNA complex for subsequent SAXS studies. We use commercially Cy5 fluorescently labelled primers or oligomers for imaging, although

radiolabelled DNA may also be used. This acts as an initial test before scale up of protein and DNA production. It is desirable to obtain a single species for SAXS experiments, however downstream deconvolution of ensembles is possible (Tria et al. 2015; Meisburger et al. 2020; Tully et al. 2021).

5. Electrophoretic Mobility-Shift Assay (EMSA) (optional)

    1. Cy5- labelled oligonucleotides containing the binding site for the TF of interest can be commercially synthesized and HPLC purified prior to DNA annealing.
    2. Mix the Cy5-labelled oligomer and unlabeled complementary strand in equimolar concentrations and perform DNA annealing as per section 2.3. Attention: Aluminum foil should be used to protect the DNA from light as the fluorophore is light-sensitive. Cover the Eppendorf tube with aluminum foil or perform annealing in the dark.
    3. Dilute the annealed dsDNA in water to 20 to 30 nM final concentration for EMSA.
    4. Mix the TF with the DNA with a constant DNA concentration of 10 nM and a varying protein concentration and incubate the complex with the DNA in binding buffer.
    5. Incubate the mixture for 1 hr. Different temperature conditions may be sampled to determine the effects of temperature on complex formation. Attention! Run the non-denaturing gel at the same temperature as for the incubation.
    6. Prepare a 5-8 % polyacrylamide gel.
    7. Prepare the gel running apparatus and fill with 0.5 x TBE.
    8. Add 50 % glycerol to the protein DNA complexes for a final glycerol concentration of 10 %.
    9. Load 5 μL of the protein–DNA complexes into the wells of the gel. The glycerol in the samples will be faintly visible when loading due to differences in refractive index.

10. Run the gel at the appropriate temperature (i.e. 4° C). If temperature dependent binding is being assayed, run the gel at the same temperature as the incubation temperature.
11. Take the gel out of the system, carefully open the glass plates and image the gel using a fluorescence imager such as a ChemiDoc or similar. Attention! Due to the low concentration of polyacrylamide the gel will be very delicate and care should be taken when removing from the gel from the glass slides.

2.2 SAXS sample preparation using sucrose for protein/DNA mixtures and complexes

As described in the introduction, SAXS data acquisition relies on scattering differences between the particles in solution and the surrounding solvent. The electron density, ρ, of pure water is 0.334 e^{-} $Å^{-3}$. However, the addition of salts, metal ions and small molecules will alter this value if they are at high enough concentration to contribute to the total electron density of the solvent (Figure 2). The ρ for the solvent with an additive (ρ_{sol}) can be calculated using the formula

$$\rho sol = (N\left(\frac{m_{add}}{MW_{add}} \times xe^{-} + \frac{m_{wat}}{MW_{wat}} \times 10\right))/ V_{final}$$

where m_{add} is the grams of additive, MW_{add} is the molecular weight of the additive, xe- is the number of electrons per molecule of additive, m_{wat} is the mass in grams of water, MW_{wat} is the molecular weight of water, 10 is the number of electrons per water molecule, N is Avogadro's number and V_{final} is the final volume of the solution. The ρ_{sol} is generally converted to the number of electrons per cubic Å. Using this equation, a 50 % sucrose additive solution with a density of 1.23 g/mL will give a ρ=0.404 e^{-} $Å^{-3}$. For many additives including sucrose, density tables are available online and V_{final} does not need to be measured. For calculating protein and DNA contributions to the total scattering the same procedure is used, however this requires measuring the final volume of the solution which may not be feasible for small sample volumes. We recommend systematically varying the

sucrose concentrations between 40-45 % to determine a concentration allowing contrast matching of the protein. We have found that 40-45 % sucrose generally matches out the protein density while allowing sufficient scattering from the electron-rich DNA molecules (Figure 3). Metal-binding proteins or cysteine rich proteins may require higher sucrose concentrations due to their higher electron density.

It should be noted that recent work has used different electron rich small molecule additives such as iohexol (5-[N-92,3-dihydroxypropyl)acetamido]-2,4,6-triiodo-N,N'-bis(2,3-dihydroxylpropylisophthalamide for contrast variation of DDM (*n*-dodecyl-β-D-maltopyranoside) micelles and these may be useful alternatives to sucrose (Gabel et al. 2019). However, the low cost of sucrose and its relative non-reactivity towards biological macromolecules makes this additive attractive for many biological applications.

2.2.1 Sample preparation with BSA test protein and DNA

For testing different sucrose concentrations, it is recommended to use a test protein to minimize the amount of sample required during the experiment. For many beamline applications bovine serum albumin (BSA) is often used as this protein is inexpensive and commercially available. Here we show how to prepare a sample of BSA, DNA and BSA plus DNA in SEC buffer. Varying concentrations of sucrose can then be tested on the individual components and the mixture of BSA plus DNA. Test sucrose concentrations to determine which outmatches the electron density of BSA in buffer while still allowing detectable scattering from DNA. This optimization protocol will allow the determination of the appropriate sucrose concentration for the target TF and TF-DNA complex. BSA and DNA concentrations tested should be near the concentrations of the TF and DNA of interest (w/vol). Attention! buffer matching is a critical step in any successful SAXS experiments and we recommend preparing a 10x excess of buffer blank for each sample to be measured.

Experimental procedure:

Test sucrose concentrations to determine which outmatches the electron density of BSA in buffer (generally ~ 40-45 % depending on BSA concentration).

1. Prepare a 55 % (~2M) sucrose solution in buffer. It may be necessary to heat the solution with stirring to prepare the stock solution of sucrose.
2. Prepare 20 mg/mL BSA in buffer. Final BSA concentration is 4 mg/mL after dilutions.
3. Prepare samples according to table (see Table 1). Attention! For each sample measured a buffer blank must be available for buffer subtraction, indicated in gray in the table. Generally, a buffer blank is run before and after each sample collection. This requires at least 2x the amount of buffer as sample. It is generally desirable to prepare more buffer than needed as SAXS data quality depends on proper buffer subtraction and variations in stock solutions or pipette may affect buffer blanks.

3. SAXS Data collection and analysis

Modern synchrotrons have automated collection robots coupled to in-house developed collection software, so the beamline data collection procedure here may vary with the synchrotron facility used. At BM29 at the European Synchrotron Radiation Facility (ESRF) the beamline automation has been designed to facilitate ease of use for novice and experienced users that enables rapid collection of samples and automatic processing. With the EBS-ESRF upgrade, the beamline benefitted with extra flux density at the sample position(Tully, Mark, et al.). This has enabled the measurement of proteins at low concentrations (<1 mg/mL) and buffers with high scattering intensity. In general, contrast matching data collections are treated no differently than normal SAXS data collections. However, it may be the case if the concentration of the samples is too low then extra exposure time might be necessary to compensate. These parameters may require user optimization or input from the SAXS beamline scientist. Before any measurements are

taken the beamline will have been set up for you by the Local Contact, they will also run calibrations, normalizing the beamline to water.

1. Samples from 2.2.1 (BSA, BSA + sucrose, DNA, DNA+sucrose) are centrifuged at 13,000 x g in a tabletop microtube centrifuge for 10 min to remove any large particulates. ~100 µL of the samples are loaded into 0.2 mL reaction tubes (these are provided at the beamline) and at least twice as much buffer for each sample, usually in 1.5 mL microcentrifuge tubes.
2. In the experimental hutch, the sample changer (SC) robot can be easily controlled using a touch screen, only two buttons are required. In the control software press "load position" and the sample table will appear below the transparent cover. Slide the cover to open and place the tubes into one of the three sample holders, these are sized to different volumes of microcentrifuge tube.
3. Press the tubes down into the holder, being careful that no tubes are sticking up, note their position.
4. Close the robots transparent cover and press "scan and park" in the software to prepare the SC robot for measurement.
5. For safety, interlock the experimental hutch using the standard procedure, as shown in the User Safety Training and by the local contact.
6. In the control hutch, the sample positions and any changes to parameters need to be determined.
7. In the beam line control software, BSXCuBE3 click on the "SC" button located on the left-hand side of the screen for the dedicated sample changer page, here you will see a schematic of the sample holders where you placed your samples. The procedure is to choose where the buffers are placed and name them, then repeat with the samples also noting which buffer is related to which sample using a handy dropdown menu before adding them to a queue. The software will be preset with standard collection protocols,

though these are easily changed, the Local Contact will guide you through this.

8. Collection parameters 50 µl sample measured for 10 frames at one second exposure time per frame at 100 % transmission and 12.5 KeV are the standard procedures with the viscosity setting set to “high” for the sucrose samples. When all samples are loaded Press “Run” to start the experiment.

NOTE: to use the synchrotron facilities you must request beam time and do this as early as possible. It will generally take up to 6 weeks for applications to be accepted and up to another 6 weeks for scheduled experiment to take place. Guidelines for access and on how to apply can be found on the synchrotron web pages. For example, in case of the ESRF: .
After an invitation for the experiment, all participants must complete a safety training and fill in the “A-form” (via the ESRF user portal) to declare all participating researchers and required safety information for their samples. It is best to discuss with the Local Contact in advance about the experiment you would like to perform to enable the correct set-up of the beamline. These procedures will vary according to synchrotron and the sample handling environment available. However, the basic protocol will be similar at different synchrotrons.

3.1 Data Analysis

The collected SAXS data is measured in terms of intensity of signal at the detector (I) at a given q value (q) in units $Å^{-1}$ or nm^{-1}. At BM29 the scattering data on the detector is automatically radially integrated. These data are then sent to an automated pipeline, FreeSAS. This first checks each frames similarity to each other frame using a correlation mapping routine, averaging together only those frames that are similar (Incardona et al. 2009; Brennich et al. 2016). This has the advantage of removing frames that may show features such as aggregation caused by radiation damage. The averaged buffers are then subtracted from the averaged samples to give a final subtracted data set for each sample.

This is handily uploaded to an online data repository, ISpyB/exi that is only accessible by the current users (De Maria Antolinos et al. 2015). All data collected are available, unsubtracted and individual frames to enable manual averaging and subtractions, if this is required. Easy to use guides on manual subtractions and primary processing of collected data are available and described in detail (Kikhney and Svergun 2015; Thompson et al. 2017; Tully et al. 2021). Below is an example of a subtracted scattering curve, the R_g calculation and Kratky plots from the automated data processing software (Figure 4A-C). Other programs such as Scatter IV allow the user to upload SAXS buffered subtracted data files (*.dat) and perform primary data analysis including Guinier analysis, normalized Kratky plots, Porod-Debye volume and D_{max} calculations with a user-friendly and intuitive interface (Tully et al. 2021). There are a number of different SAXS data analysis programs available with the same capabilities and may also be used including BioXTAS RAW, ATSAS package and US-SOMO (Franke et al. 2017; Hopkins et al. 2017; Brookes and Rocco 2018).

3.2 Contrast matching

After collecting the data from the BSA, DNA and sucrose samples, contrast matching conditions may be determined. A contrast matched protein will show little to no scattering, where the scattering intensity of the buffer is greater or equivalent to the scattering of the protein. This is characterized by a reduction of the initial high intensity peak seen in a scattering profile at 0 % sucrose concentrations. Taking the SAXS datasets at each contrast matching point (0 %, 22 %, 33 % and 44 % sucrose) and overlaying them (Figure 4D) it can be clearly seen that at 44 % sucrose the scattering of the protein has been matched out as the scattering profile is flat. Ideally, a second experiment might be carried out to define more closely the match point testing between 33 % and 44 %. It is important to note that the scattering intensity from all components of the solution (i.e. DNA) will exhibit reduced intensity due to the added sucrose in the solution. To maximize the scattering from DNA, the minimum concentration of sucrose to match out the protein should be used.

3.3 Contrast variation controls

When contrast matching out the protein it is necessary that the scattering from the DNA is still measurable and not matched out together with the protein. Initially, when overlaying the curves from DNA in 0 % sucrose buffer and the DNA in 44 % sucrose (Figure 5A) we can visually see the scattering intensity of the DNA is still present albeit at lower intensity, caused by the high electron density of the sucrose. A second measure is to see if the Rg from both the DNA's are similar (17.9 Å for DNA 0 % and 17.8 Å for DNA 44 %). A final test for similarity is to take a ratio of the two curves. We recommend the SAXS data analysis program Scatter IV for this (https://bl1231.als.lbl.gov/scatter/). Easy to use published protocols are available to guide the novice user through the upload of data and data analysis steps (Tully et al. 2021). Comparison of curves can be observed from the "ratio" button in Scatter IV (Figure 5B). Here the plot illustrates the ratio between the two DNA's, the greater the deviation from the line, the less similar the curves. In this example the curves are almost identical. Any differences at high-q (> 0.3 Å) is representative of the weak scattering of the DNA in 44 % sucrose and not indicative of a structural difference.

3.4 BSA-DNA Contrast variation

After these controls have been performed in which the protein scattering has been matched out and the effects of the high sucrose buffer on DNA have been determined (in this case there is no observable change in DNA structure in high sucrose), the mixture of protein and DNA can be used in the high sucrose buffer. The scattering profiles of BSA and BSA:DNA, with 0 % sucrose are noticeably different (Figure 6A). This is due to the presence of protein and DNA in the same solution, forming a heterogeneous mixture of molecules which both scatter the incident X-rays to give a single scattering curve. With the addition of the contrast matching sucrose at 44 % to the BSA:DNA mixture, the scattering intensity of the protein is reduced to almost zero leaving only the scattering intensity of the DNA remaining (Figure 6B). To verify the scattering from the BSA:DNA in 44 % sucrose complex is from the DNA alone, we compare the scattering to the DNA in 0 % sucrose buffer as above (Figure 6C). We find that the Rg increased slightly to 18.5 for the BSA:DNA mixture,

but this can be attributed to the lower intensity scattering with the addition of the sucrose. When taking the ratio of the two curves (Figure 6D) the curve is flat as expected until excess noise from the low intensity scattering is seen.

These experiments demonstrate that the scattering of protein can be successfully matched out using sucrose and that in a solution of protein and DNA components, the scattering of the higher electron density material, in this case DNA, is still observable. In addition, comparisons of DNA scattering curves and the ratio of scattering can be used to detect potential differences in the size and/or shape of the DNA in buffer and high sucrose buffers with or without protein present.

3.5 Transcription factor contrast matching using LUX

The TF of interest (here we use LUX ARRYTHMO as an example) was purified as described. In this second experiment LUX, LUX and DNA, LUX and DNA and sucrose scattering curves were measured, using the sucrose range determined with BSA in the experiment above. SAXS data are collection as per BSA (see section 2.2). Note that BSA and LUX proteins have a similar electron density at the same concentration in mg/mL. While BSA has about twice the number of electrons per molecule, it has a molecular weight approximately twice that of LUX (see Table 2 and 3 for an example).

LUX concentrations up to 4 mg/mL will be matched out using the 44 % sucrose buffer determined for BSA contrast matching. It should be noted that most proteins will be successfully matched out in this range of sucrose. However, in cases of metal binding proteins or bound electron dense cofactors the concentration of sucrose may need to be increased.

3.6 Sample preparation of the TF, LUX, and LUX-DNA complexes using contrast variation

1. Calculate the molarity of protein and DNA. For this experiment LUX is 150 µM.
2. Dilute the DNA to 150 µM by mixing 15 µL DNA with 35 µL water to be able to mix LUX and DNA in a 1:1 ratio.
3. Mix the components according to the table (Table 4). Use 55 % sucrose stock solution as for BSA.
4. Perform data collection as described in **2.2.2**

3.7 Transcription factor contrast matching

From the BSA contrast matching we saw BSA and DNA not interacting, creating a heterogeneous mixture exemplified by their scattering profiles. Transcription factors by their nature bind DNA. Overlaying the curves of LUX alone and LUX with DNA in 0 % sucrose shows a slight change in the scattering curves, suggesting that there is no free DNA and that the DNA bound to the LUX a small effect on the structure of the complex vs. LUX protein alone (Figure 7A and B).

Examination of the scattering profiles of LUX alone and the LUX-DNA complex in 44 % sucrose demonstrates that LUX protein no longer contributes to the scattering profile and only DNA alone can be observed (Figure 7C). Weak scattering intensity is observed for the DNA alone in the LUX:DNA 44 % sucrose buffer, which shows a good overlay in the low-q area to 0.1 Å with DNA alone. When the matched-out LUX:DNA is overlaid with DNA (Figure 7D to F) the shape of the curve is representative of the DNA shape, suggesting there is no change in the DNA conformation upon complex formation.

Taken together these data demonstrate that the DNA does not undergo major structural changes upon complex formation. Examination of the scattering curves of LUX and LUX:DNA and comparison of the auto-processed data (R_g, Kratky, D_{max}) shows a small elongation of the LUX:DNA complex and an increase in the rigidity of the complex versus the protein alone.

Summary of procedures

Prepare test protein, protein of interest and DNA.

Define necessary match point for test protein.

Prepare protein of interest in the matched buffer.

Prepare DNA in its equivalent buffer.

Measure batch SAXS experiment – protein + DNA and controls of protein and DNA alone.

Primary SAXS data analysis (automatic data processing pipeline OR user manual processing).

Overlay DNA with protein and without to see if there are changes in the shape of curves that will relate to changes in DNA shape or protein shape.

EXPECTED OUTCOMES

Performing the BSA sucrose gradient provides values at which the sucrose concentration outmatches the protein signal in the SAXS curve. Here we can show that 44 % sucrose solution in the BSA sample at 4 mg/mL leads to a close to flat intensity plot (Figure 4D). The same sucrose concentration outmatches a test TF, LUX, at a similar concentration (Figure 7C). In contrast, scattering from DNA is observable in the 44 % sucrose solutions for both BSA and LUX.

Comparisons between DNA alone and DNA in complex with the TF of interest will allow the determination of major changes in DNA conformation due to complex formation using SAXS. In addition, data measured from the TF alone, TF-DNA and contrast matched TF-DNA will aid in interpretation of scattering curves and changes in the size and shape of the molecule due to either protein or DNA. Using this sample preparation and data collection pipeline, the user will be able to distinguish between protein and DNA in a mixture or complex and whether the DNA has changed in shape relative to the unbound form. Standard downstream data analysis should be performed to compare the size and shape

of the complexes using SAXS protocols described in detail elsewhere (Rambo 2015; Grant 2018; Manalastas-Cantos et al. 2021; Tully et al. 2022).

Conclusion

SAXS offers a complementary solution-state technique to high resolution structural methods such as NMR and protein crystallography for the study of protein-nucleic acid complexes. However, while a drawback of SAXS is the low-resolution data generated the ability to use contrast variation provides a relatively simple way to determine the contributions from protein and DNA in a complex or mixture. It should be noted that most modern bioSAXS beamlines at synchrotron sources have the high flux and liquid handing robotic sample environments required for these types of experiments. While we present here data measured under 0 % and 44 % sucrose conditions at a single temperature, this protocol is easily adaptable to measuring samples with different additives, buffer conditions (ionic strengths, pH) and different temperatures. Sampling different physicochemical variables using contrast matching offers an accessible way to examine TF binding under different conditions. This offers a feasible way to study TFs that exhibit differential binding as a function of pH, ionic strength, and temperature and to determine whether protein and/or DNA structural changes occur upon complex formation.

OPTIMIZATION AND TROUBLESHOOTING

Poor TF expression, poor DNA binding

Prior to any SAXS experiment, a stable TF-DNA complex must be formed and purified. This may require the use of different expression systems (prokaryotic and eukaryotic) for TF expression and purification protocol optimization. Expression temperature and time, buffer pH and salt concentration may need to be systematically tested to determine the proper conditions for TF purification. We have found that for different TF families including MADS and MYB domain TFs, a high pH buffer (9-10.5) and high salt concentrations (500 mM-1 M) during protein purification result in higher yields of active and soluble protein. For complex formation with DNA, buffer pH and salt concentration are reduced either via dialysis in the presence of DNA or via dilution. A second critical step

in sample preparation is the verification that the TF of interest is active, i.e. binds DNA. EMSAs are a fast and easy way to test TF-DNA binding, alter buffer conditions and to obtain an estimate of the k_d. These steps should be performed before scale-up of TF-DNA complex formation. Milligram quantities of TF-DNA complex should be purified by FPLC prior to any SAXS experiment for best results.

Problem signal to noise ratio

The signal to noise ratio might be poor in the high sucrose environment. To obtain better data it might be beneficial to use higher concentrations of protein and DNA and to experimentally determine the exact match point of sucrose and the protein of interest. The user must keep in mind that SAXS data quality highly depends on the sample quality and monodispersity. Aggregation at higher protein concentrations may occur and this will negatively impact the quality of the data collected and interpretation of the final models. Online purification systems maybe used during the SAXS experiment, however these are generally not compatible with high viscosity buffers. Alternatively, new chemical components might be tested, which might buffer match at lower concentrations(Gabel et al. 2019).

ACKNOWLEDGMENTS

We acknowledge financial support for the project from the ANR (ANR-19-CE20-0021) grant. We thank the ESRF for the SAXS beam time. This work used the platforms of the Grenoble Instruct-ERIC center (ISBG; UMS 3518 CNRS-CEA-UGA-EMBL) within the Grenoble Partnership for Structural Biology (PSB), supported by FRISBI (ANR-10-INBS-05-02) and GRAL, financed within the University Grenoble Alpes graduate school (Ecoles Universitaires de Recherche) CBH-EUR-GS (ANR-17-EURE-0003).

DISCLOSURES

The authors have nothing to disclose.

References

Andrabi M, Mizuguchi K, Ahmad S (2014) Conformational changes in DNA-binding proteins: Relationships with precomplex features and contributions to specificity and stability. Proteins. https://doi.org/10.1002/prot.24462

Ballauff M (2001) SAXS and SANS studies of polymer colloids. Current Opinion in Colloid & Interface Science 6:132–139. https://doi.org/10.1016/S1359-0294(01)00072-3

Bolze J, Ballauff M, Kijlstra J, Rudhardt D (2003) Application of Small-Angle X-Ray Scattering as a Tool for the Structural Analysis of Industrial Polymer Dispersions. Macromol Mater Eng 288:495–502. https://doi.org/10.1002/mame.200390046

Bolze J, Hörner KD, Ballauff M (1996) Adsorption of the Nonionic Surfactant Triton X-405 on Polystyrene Latex Particles As Monitored by Small-Angle X-ray Scattering. Langmuir 12:2906–2912. https://doi.org/10.1021/la951073c

Brennich ME, Kieffer J, Bonamis G, De Maria Antolinos A, Hutin S, Pernot P, Round A (2016) Online data analysis at the ESRF bioSAXS beamline, BM29. Journal of Applied Crystallography 49:203–212. https://doi.org/10.1107/S1600576715024462

Brookes E, Rocco M (2018) Recent advances in the UltraScan SOlution MOdeller (US-SOMO) hydrodynamic and small-angle scattering data analysis and simulation suite. Eur Biophys J 47:855–864. https://doi.org/10.1007/s00249-018-1296-0

Brosey CA, Tainer JA (2019) Evolving SAXS versatility: solution X-ray scattering for macromolecular architecture, functional landscapes, and integrative structural biology. Curr Opin Struct Biol 58:197–213. https://doi.org/10.1016/j.sbi.2019.04.004

Burke JE, Butcher SE (2012) Nucleic acid structure characterization by small angle X-ray scattering (SAXS). Curr Protoc Nucleic Acid Chem CHAPTER:Unit7.18. https://doi.org/10.1002/0471142700.nc0718s51

Chen Y, Pollack L (2016) SAXS Studies of RNA: structures, dynamics, and interactions with partners. Wiley Interdiscip Rev RNA 7:512–526. https://doi.org/10.1002/wrna.1349

Chen Y, Tokuda JM, Topping T, Meisburger SP, Pabit SA, Gloss LM, Pollack L (2017) Asymmetric unwrapping of nucleosomal DNA propagates asymmetric opening and dissociation of the histone core. Proc Natl Acad Sci USA 114:334–339. https://doi.org/10.1073/pnas.1611118114

Chu B, Hsiao BS (2001) Small-Angle X-ray Scattering of Polymers. Chem Rev 101:1727–1762. https://doi.org/10.1021/cr9900376

Chu X, Liu F, Maxwell BA, Wang Y, Suo Z, Wang H, Han W, Wang J (2014) Dynamic Conformational Change Regulates the Protein-DNA Recognition: An Investigation on Binding of a Y-Family Polymerase to Its Target DNA. PLOS Computational Biology 10:e1003804. https://doi.org/10.1371/journal.pcbi.1003804

Classen S, Hura GL, Holton JM, Rambo RP, Rodic I, McGuire PJ, Dyer K, Hammel M, Meigs G, Frankel KA, Tainer JA (2013) Implementation and performance of SIBYLS: a dual endstation small-angle X-ray scattering and macromolecular crystallography beamline at the Advanced Light Source. Journal of Applied Crystallography 46:1–13. https://doi.org/10.1107/S0021889812048698

De Maria Antolinos A, Pernot P, Brennich ME, Kieffer J, Bowler MW, Delageniere S, Ohlsson S, Malbet Monaco S, Ashton A, Franke D, Svergun D, McSweeney S, Gordon E, Round A (2015) ISPyB for BioSAXS, the gateway to user autonomy in solution scattering experiments. Acta crystallographica Section D, Biological crystallography 71:76–85. https://doi.org/10.1107/S1399004714019609

Dingenouts N, Ballauff M (1993) [No title found]. Acta Polym 44:178–183. https://doi.org/10.1002/actp.1993.010440402

Dwivedi D, Lepkova K (2017) SAXS and SANS Techniques for Surfactant Characterization: Application in Corrosion Science

Ezer D, Jung JH, Lan H, Biswas S, Gregoire L, Box MS, Charoensawan V, Cortijo S, Lai X, Stockle D, Zubieta C, Jaeger KE, Wigge PA (2017) The evening complex coordinates environmental and endogenous signals in Arabidopsis. Nat Plants 3:17087. https://doi.org/10.1038/nplants.2017.87

Fernandez RM, Riske KA, Amaral LQ, Itri R, Lamy MT (2008) Influence of salt on the structure of DMPG studied by SAXS and optical microscopy. Biochimica et Biophysica Acta (BBA) - Biomembranes 1778:907–916. https://doi.org/10.1016/j.bbamem.2007.12.005

Franke D, Petoukhov MV, Konarev PV, Panjkovich A, Tuukkanen A, Mertens HDT, Kikhney AG, Hajizadeh NR, Franklin JM, Jeffries CM, Svergun DI (2017) ATSAS 2.8: a comprehensive data analysis suite for small-angle scattering from macromolecular solutions. J Appl Crystallogr 50:1212–1225. https://doi.org/10.1107/S1600576717007786

Gabel F, Engilberge S, Pérez J, Girard E (2019) Medical contrast media as possible tools for SAXS contrast variation. IUCrJ 6:521–525. https://doi.org/10.1107/S2052252519005943

Garcia-Diez R, Sikora A, Gollwitzer C, Minelli C, Krumrey M (2016) Simultaneous size and density determination of polymeric colloids by continuous contrast variation in small angle X-ray scattering. European Polymer Journal 81:641–649. https://doi.org/10.1016/j.eurpolymj.2016.01.012

Grant TD (2018) Ab initio electron density determination directly from solution scattering data. Nat Methods 15:191–193. https://doi.org/10.1038/nmeth.4581

Hickl P, Ballauff M, Jada A (1996) Small-Angle X-ray Contrast-Variation Study of Micelles Formed by Poly(styrene)−Poly(ethylene oxide) Block Copolymers in Aqueous Solution. Macromolecules 29:4006–4014. https://doi.org/10.1021/ma951480v

Hopkins JB, Gillilan RE, Skou S (2017) BioXTAS RAW: improvements to a free open-source program for small-angle X-ray scattering data reduction and analysis. J Appl Crystallogr 50:1545–1553. https://doi.org/10.1107/S1600576717011438

Hura GL, Budworth H, Dyer KN, Rambo RP, Hammel M, McMurray CT, Tainer JA (2013) Comprehensive macromolecular conformations mapped by quantitative SAXS analyses. Nat Methods. https://doi.org/10.1038/nmeth.2453

Hutin S, Brennich M, Maillot B, Round A (2016) Online ion-exchange chromatography for small-angle X-ray scattering. Acta Crystallogr D Struct Biol 72:1090–1099. https://doi.org/10.1107/S2059798316012833

Incardona MF, Bourenkov GP, Levik K, Pieritz RA, Popov AN, Svensson O (2009) EDNA: a framework for plugin-based applications applied to X-ray experiment online data analysis. J Synchrotron Radiat 16:872–9. https://doi.org/10.1107/S0909049509036681

Jumper J, Evans R, Pritzel A, Green T, Figurnov M, Ronneberger O, Tunyasuvunakool K, Bates R, Žídek A, Potapenko A, Bridgland A, Meyer C, Kohl SAA, Ballard AJ, Cowie A, Romera-Paredes B, Nikolov S, Jain R, Adler J, Back T, Petersen S, Reiman D, Clancy E, Zielinski M, Steinegger M, Pacholska M, Berghammer T, Bodenstein S, Silver D, Vinyals O, Senior AW, Kavukcuoglu K, Kohli P, Hassabis D (2021) Highly accurate protein structure prediction with AlphaFold. Nature 596:583–589. https://doi.org/10.1038/s41586-021-03819-2

Kidd PS, Proctor J (2001) Why plants grow poorly on very acid soils: are ecologists missing the obvious? Journal of Experimental Botany 52:791–799. https://doi.org/10.1093/jexbot/52.357.791

Kikhney AG, Svergun DI (2015) A practical guide to small angle X-ray scattering (SAXS) of flexible and intrinsically disordered proteins. FEBS Letters 589:2570–2577. https://doi.org/10.1016/j.febslet.2015.08.027

Kiselev MA, Lesieur P, Kisselev AM, Lombardo D, Killany M, Lesieur S (2001) Sucrose solutions as prospective medium to study the vesicle structure: SAXS and SANS study. Journal of Alloys and Compounds 328:71–76. https://doi.org/10.1016/S0925-8388(01)01348-2

Kiselev MA, Lombardo D (2017) Structural characterization in mixed lipid membrane systems by neutron and X-ray scattering. Biochim Biophys Acta Gen Subj 1861:3700–3717. https://doi.org/10.1016/j.bbagen.2016.04.022

Manalastas-Cantos K, Konarev PV, Hajizadeh NR, Kikhney AG, Petoukhov MV, Molodenskiy DS, Panjkovich A, Mertens HDT, Gruzinov A, Borges C, Jeffries CM, Svergun DI, Franke D (2021) ATSAS 3.0: expanded functionality and new tools for small-angle scattering data analysis. J Appl Cryst 54:343–355. https://doi.org/10.1107/S1600576720013412

Meisburger SP, Xu D, Ando N (2020) REGALS: a general method to deconvolve X-ray scattering data from evolving mixtures. 2020.12.06.413997

Naruse K, Eguchi K, Akiba I, Sakurai K, Masunaga H, Ogawa H, Fossey JS (2009) Flexibility and Cross-Sectional Structure of an Anionic Dual-Surfactant Wormlike Micelle Explored with Small-Angle X-ray Scattering Coupled with Contrast Variation Technique. J Phys Chem B 113:10222–10229. https://doi.org/10.1021/jp9019415

Nusinow DA, Helfer A, Hamilton EE, King JJ, Imaizumi T, Schultz TF, Farré EM, Kay SA (2011) The ELF4-ELF3-LUX Complex Links the Circadian Clock to Diurnal Control of Hypocotyl Growth. Nature 475:398–402. https://doi.org/10.1038/nature10182

Pabo, Carl O. S Robert T (1992) Transcription Factors: Structural Families and Principles of DNA Recognition. Annual Review of Biochemistry 61:1053–1095

Poddar S, Chakravarty D, Chakrabarti P (2018) Structural changes in DNA-binding proteins on complexation. Nucleic Acids Res 46:3298–3308. https://doi.org/10.1093/nar/gky170

Putnam CD, Hammel M, Hura GL, Tainer JA (2007) X-ray solution scattering (SAXS) combined with crystallography and computation: defining accurate macromolecular structures, conformations and assemblies in solution. Q Rev Biophys 40:191–285. https://doi.org/10.1017/S0033583507004635

Rambo RP (2015) Chapter Twelve - Resolving Individual Components in Protein–RNA Complexes Using Small-Angle X-ray Scattering Experiments. In: Woodson SA, Allain FHT (eds) Methods in Enzymology. Academic Press, pp 363–390

Rambo RP, Tainer JA (2013a) Super-resolution in solution x-ray scattering and its applications to structural systems biology. Annu Rev Biophys 42:415–41. https://doi.org/10.1146/annurev-biophys-083012-130301

Rambo RP, Tainer JA (2010a) Bridging the solution divide: comprehensive structural analyses of dynamic RNA, DNA, and protein assemblies by small-angle X-ray scattering. Curr Opin Struct Biol 20:128–37. https://doi.org/10.1016/j.sbi.2009.12.015

Rambo RP, Tainer JA (2010b) Improving small-angle X-ray scattering data for structural analyses of the RNA world. RNA 16:638–46. https://doi.org/10.1261/rna.1946310

Rambo RP, Tainer JA (2013b) Accurate assessment of mass, models and resolution by small-angle scattering. Nature 496:477–81. https://doi.org/10.1038/nature12070

Round A, Brown E, Marcellin R, Kapp U, Westfall CS, Jez JM, Zubieta C (2013) Determination of the GH3.12 protein conformation through HPLC-integrated SAXS measurements combined with X-ray crystallography. Acta Crystallogr D Biol Crystallogr 69:2072–80. https://doi.org/10.1107/S0907444913019276

Silva CS, Nayak A, Lai X, Hutin S, Hugouvieux V, Jung J-H, López-Vidriero I, Franco-Zorrilla JM, Panigrahi KCS, Nanao MH, Wigge PA, Zubieta C (2020) Molecular mechanisms of Evening Complex activity in Arabidopsis. Proc Natl Acad Sci U S A 117:6901–6909. https://doi.org/10.1073/pnas.1920972117

Thompson MK, Ehlinger AC, Chazin WJ (2017) Chapter Three - Analysis of Functional Dynamics of Modular Multidomain Proteins by SAXS and NMR. In: Eichman BF (ed) Methods in Enzymology. Academic Press, pp 49–76

Tria G, Mertens HDT, Kachala M, Svergun DI (2015) Advanced ensemble modelling of flexible macromolecules using X-ray solution scattering. IUCrJ 2:207–217. https://doi.org/10.1107/S205225251500202X

Tully, Mark, et al. BioSAXS at European Synchrotron Radiation Facility - Extremely Brilliant Source – BM29 with an upgraded source, detector, robot, sample environment, data collection and analysis software. J Synchrotron Rad in press

Tully MD, Tarbouriech N, Rambo RP, Hutin S (2021) Analysis of SEC-SAXS data via EFA deconvolution and Scatter. JoVE (Journal of Visualized Experiments) e61578. https://doi.org/10.3791/61578

Wolberger C (1993) Transcription factor structure and DNA binding. Current Opinion in Structural Biology 3:3–10. https://doi.org/10.1016/0959-440X(93)90194-P

Wolberger C (2021) How structural biology transformed studies of transcription regulation. Journal of Biological Chemistry 296. https://doi.org/10.1016/j.jbc.2021.100741

Tables

Table 1. Example of contrast matching SAXS sample preparation using BSA.

Sample	BSA	BSA, 22% sucrose solution	BSA, 33% sucrose solution	BSA, 44% sucrose solution	DNA	DNA, 44% sucrose	BSA, DNA, 44% sucrose
Protein	20 µL	20 µL	20 µL	20 µL	-	-	10 µL
DNA	-	-	-	-	10 µL	10 µL	-
Sucrose	-	40 µL	60 µL	80 µL	-	80 µL	80 µL
Buffer	80 µL	40 µL	20 µL	-	90 µL	10 µL	-
water	-	-	-	-	-	-	10 µL
Final volume	**100 µL**	**100 µL**	**100 µL**	**100 µL**	**100 µL**	**100 µL**	**100 µL**

Buffer	Buffer BSA	22% sucrose solution	33% sucrose solution	44% sucrose solution	Buffer DNA	Buffer DNA, 44% sucrose	Buffer BSA, DNA, 44% sucrose
Protein	-	-	-	-	-	-	-
DNA	-	-	-	-	-	-	-
Sucrose	200 µL	400 µL	600 µL	800 µL	-	800 µL	800 µL
Buffer	800 µL	600 µL	400 µL	200 µL	900 µL	100 µL	100 µL
water	-	-	-	-	100 µL	100 µL	100 µL
Final volume	**1 mL**	**1 mL**	**1 mL**	**1 mL**	**1 mL**	**1 mL**	**1 mL**

Table 2. Calculation of the number of electrons in BSA. BSA has 37020 electron per molecule.

BSA	Atoms	Electrons/atom	Summe
C	3071	6	18426
H	4826	1	4826
N	816	7	5712
O	927	8	7416
S	40	16	640
			37020

Table 3. Calculation of the number of electrons in LUX. LUX has 18448 electron per molecule.

LUX	Atoms	Electrons/atom	Summe
C	1470	6	8820
H	2285	1	2285
N	441	7	3087
O	500	8	4000
S	16	16	256
			18448

Table 4. Example of contrast matching SAXS sample preparation using LUX.

Sample	LUX	LUX, 44% sucrose	LUX, DNA	LUX, DNA, 44% sucrose
Protein	10 µL	10 µL	10 µL	10 µL
DNA	-	-	10 µL	10 µL
Sucrose	-	80 µL	-	80 µL
Buffer	80 µL	-	80 µL	-
water	10 µL	10 µL	-	-

Final volume	**100 µL**	**100 µL**	**100 µL**	**100 µL**

Buffer	LUX buffer	Buffer LUX, 44% sucrose	Buffer LUX, DNA,	Buffer LUX, DNA, 44% sucrose
Protein	-	-	-	-
DNA	-	-	-	-
Sucrose	-	800 µL		800 µL
Buffer	900 µL	100 µL	900 µL	100 µL
water	100 µL	100 µL	100 µL	100 µL
Final volume	**1 mL**	**1 mL**	**1 mL**	**1 mL**

Figure legends

Figure 1. AlphaFold model of LUX ARRYTHMO. The DNA-binding MYB domain is shown in red and corresponds to the crystallized domain available in the PDB (PDB 6QEC). Predicted regions are shown in gray. A large portion of the protein is predicted to exhibit little secondary structure and is likely highly flexible.

Figure 2. Graph showing electron density as a function of sucrose concentration. The dotted line shows approximate DNA/RNA electron density in solution. Protein electron density generally ranges between 0.41-0.43 depending on protein concentration and is shown in light blue. Sucrose electron density is shown in light yellow. Figure adapted from Gabel, 2019.

Figure 3. Schematic demonstrating how contrast variation masks protein electron density. Left, protein in red and DNA in green both contribute to observed scattering in buffer without contrast agent. Right, addition of sucrose or other additives matches out the

scattering from protein (light red) leaving only the scattering from DNA detected in the SAXS experiment.

Figure 4. Automated pipeline output and contrast matching of BSA. A-C show the automated output of FreeSAS for BSA at 0 % sucrose. A. I vs q scattered intensity plot after buffer subtraction B. The Guinier plot from FreeSAS is used to provide an automatic calculation of the Rg and an estimate of the I_0. C. The Kratky plot calculation provides information as to the conformation of the molecule and whether the molecule is globular, extended or highly flexible. In the case of BSA the protein is globular due to the bell-shaped Gaussian peak in the Kratky plot. In D, the scattering intensity curves for BSA at 0 % sucrose (light blue) and increasing concentrations of sucrose 22, 33 and 44 % (colored from light to dark) are overlaid using Scatter IV and show the scattering intensity decreasing with increasing contrast agent until the protein is masked out as shown by the flat scattering curve at 44 % sucrose.

Figure 5. DNA contrast control. A. Scattering intensity curves of DNA in 0 % sucrose (dark green) and DNA in 44 % sucrose (light green) overlaid show no difference to the scattering profile. Differences at high q values are due to noise in the high background sucrose buffer. B. When the ratio of the two curves is taken the flat line shows the sucrose is having no effect on the DNA structure.

Figure 6. BSA Contrast variation. A. Scattering intensity curves for BSA (dark blue) and BSA:DNA mixture (light blue) show distinctly different profiles B. With the addition of 44 % sucrose the scatting intensity decreases for BSA (dark blue curve) and the curve is almost flat. For the BSA:DNA mixture in 44 % sucrose, the scattering curve (cyan) is dominated by the scatting intensity of the DNA. C. The DNA in 0 % sucrose buffer (green) and BSA:DNA in 44 % sucrose are overlaid showing the scattering profiles are similar. D. The ratio of the DNA curves from C, are taken and shown in D. These data demonstrate that the observed scattering of BSA:DNA in 44 % sucrose is due to the DNA alone and that

the DNA conformation in 0 % and 44 % sucrose is not detectably affected by the different buffers.

Figure 7. LUX Contrast variation. A. The scattering intensity curves for LUX (magenta) and LUX:DNA complex (pink) show similar profiles with only a small change visible, highlighted in a zoomed in region of the curves in B. With the addition of 44 % sucrose C the scatting intensity for LUX decreases (magenta) leaving only the weak scatting intensity of the DNA (pink). D. The DNA in 0 % buffer (green) and LUX:DNA in 44 % sucrose (pink) are overlaid showing the scattering profiles are similar though the complex DNA is at much lower scattering intensity, the range from 0 to 0.15 q is zoomed in to highlight the similarity E. In F the ratio of the DNA curves from D further show the similarity in the scattering profiles. These results indicate that the DNA does not undergo any major conformational changes upon LUX binding. Differences in the conformation of the complex versus the individual components will be dominated by changes in the protein conformation.

Figure 1. Predicted structure of LUX ARRYTHMO. The DNA-binding MYB domain (PBD 6QEC) is shown in red and the predicted regions shown in gray. Model obtained by AlphaFold.

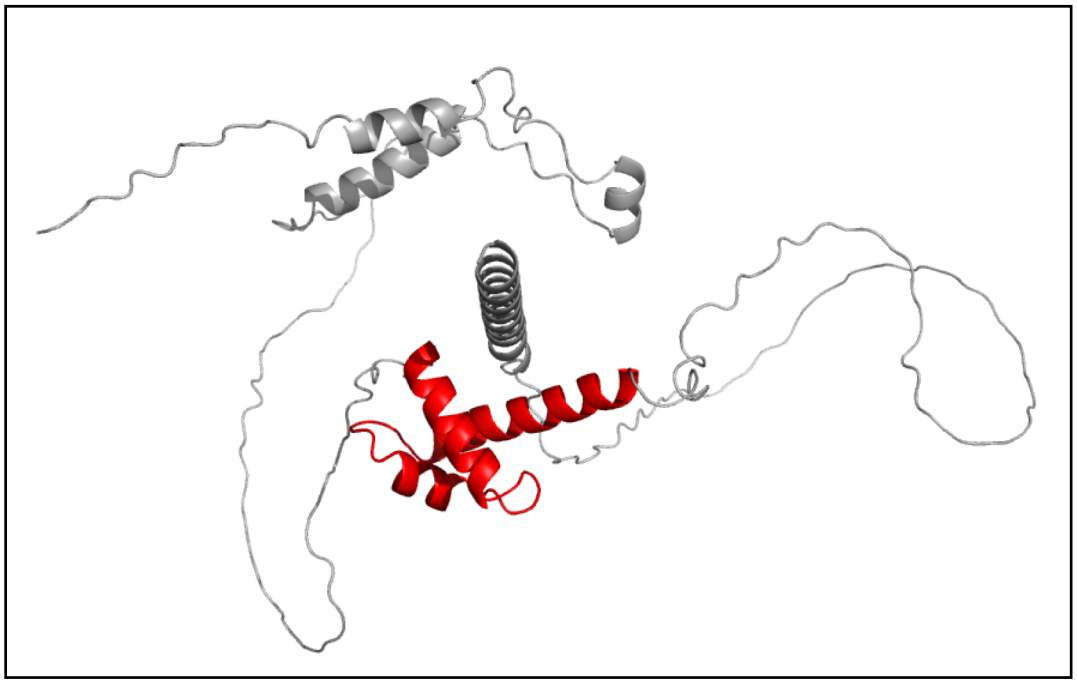

Figure 2. Graph showing electron density as a function of sucrose concentration. The dotted line shows approximate DNA/RNA electron density in solution. Protein electron density generally ranges between 0.41-0.43 depending on protein concentration and is shown in light blue. Sucrose electron density is shown in light yellow. Figure adapted from Gabel, 2019.

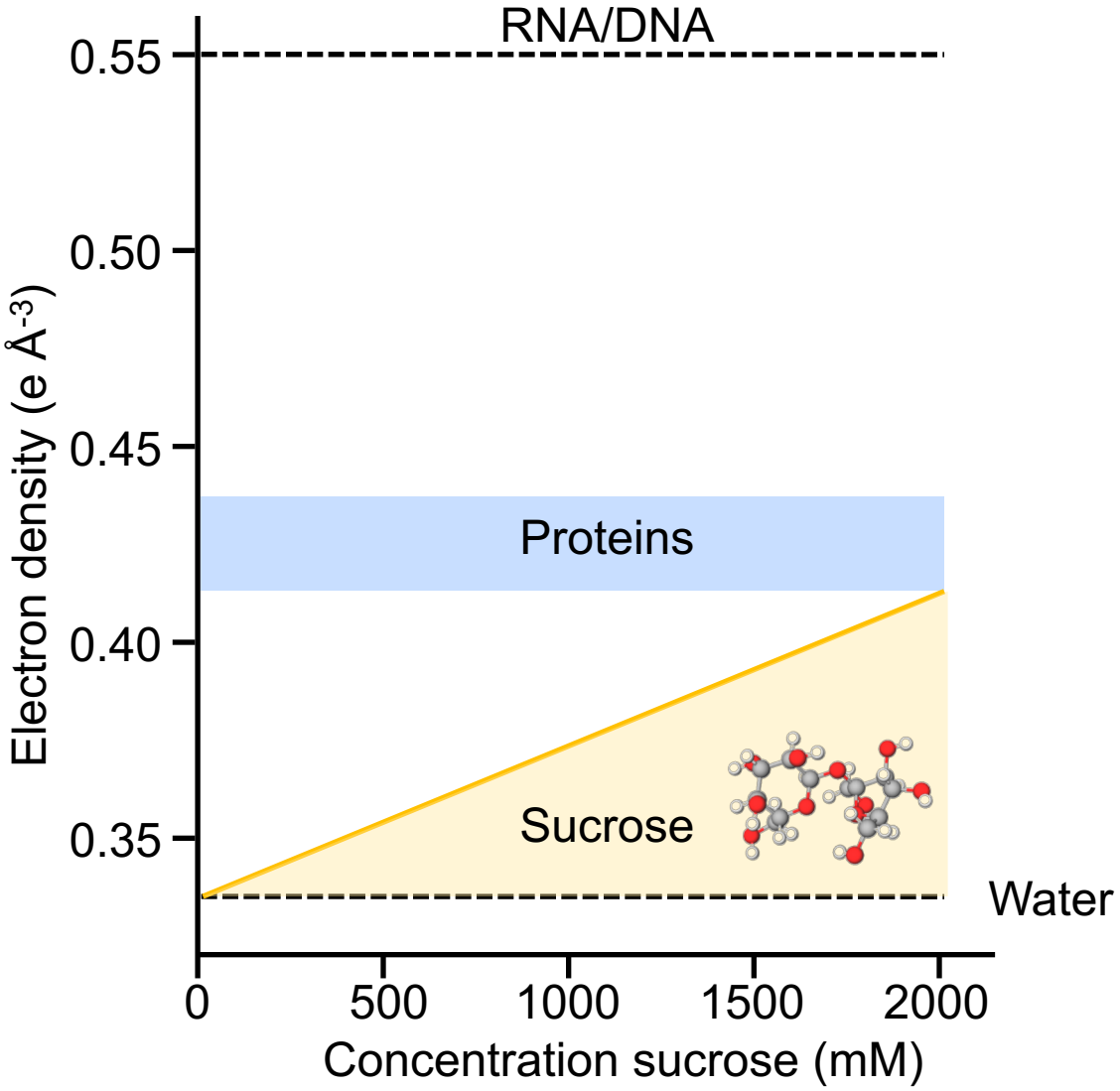

Figure 3. Contrast variation masks protein electron density. Left, protein in red and DNA in green both contribute to observed scattering in buffer without contrast agent. Right, addition of sucrose or other additives (rose) matches out the scattering from protein leaving only the scattering from DNA detected in the experiment.

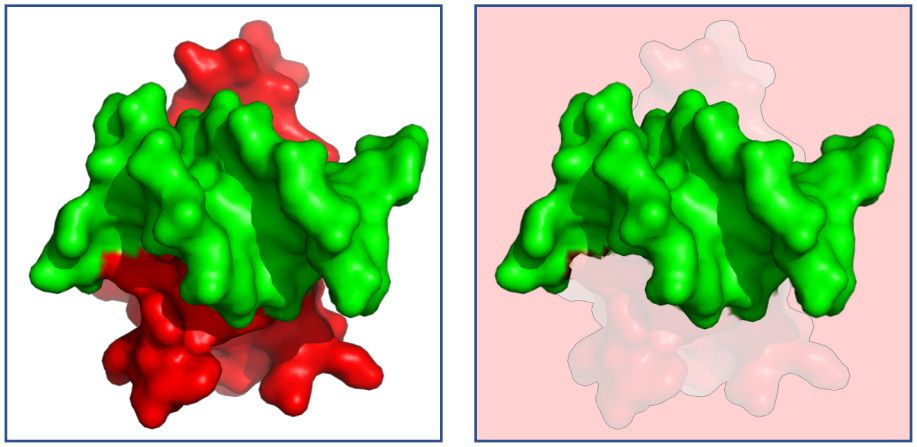

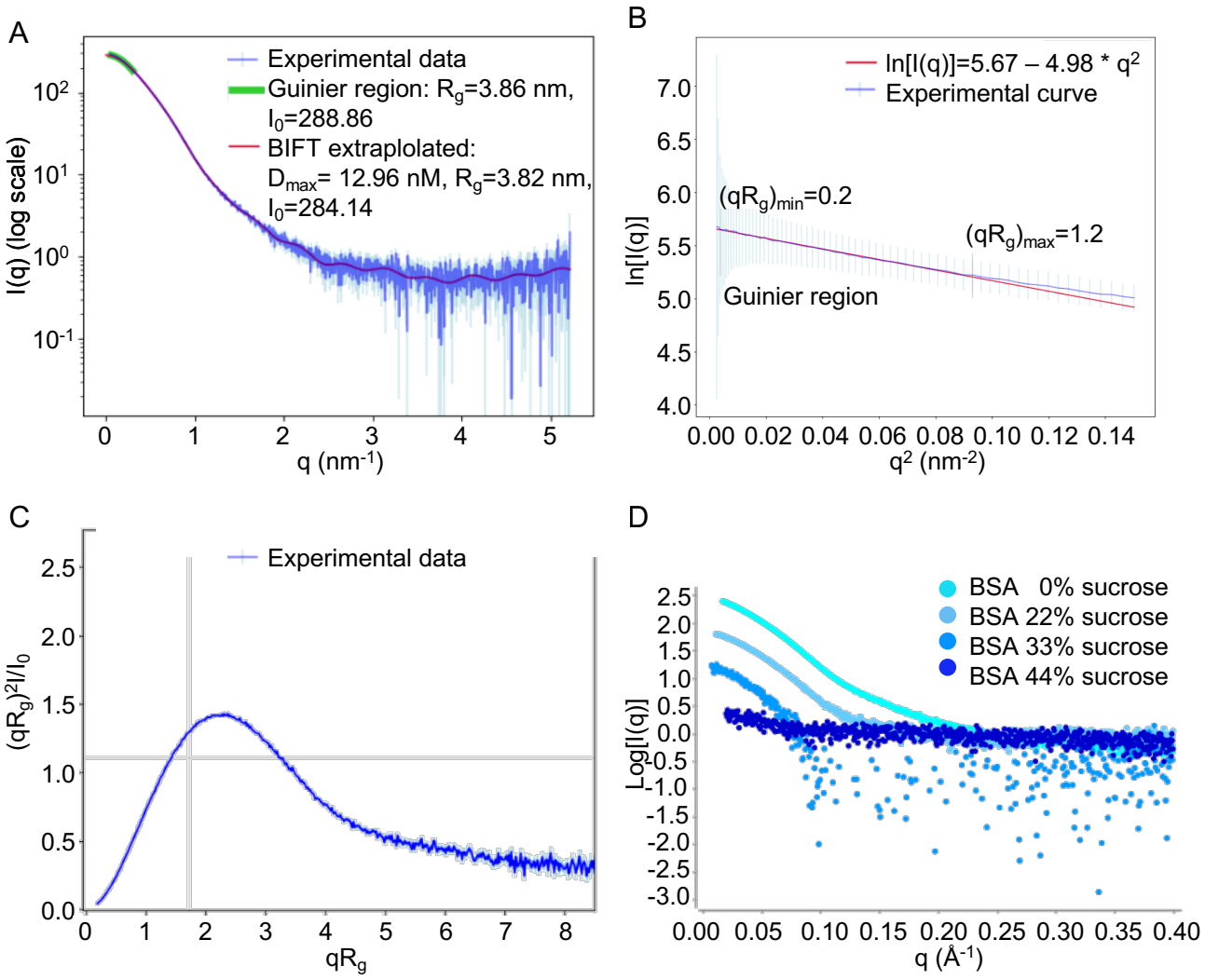
A
Experimental data
Guinier region: R_g=3.86 nm, I_0=288.86
BIFT extraplolated: D_{max}= 12.96 nM, R_g=3.82 nm, I_0=284.14
I(q) (log scale)
q (nm^{-1})
B
ln[I(q)]=5.67 – 4.98 * q^2
Experimental curve
$(qR_g)_{min}$=0.2
$(qR_g)_{max}$=1.2
Guinier region
ln[I(q)]
q^2 (nm^{-2})
C
Experimental data
$(qR_g)^2I/I_0$
qR_g
D
BSA 0% sucrose
BSA 22% sucrose
BSA 33% sucrose
BSA 44% sucrose
Log[I(q)]
q (Å^{-1})

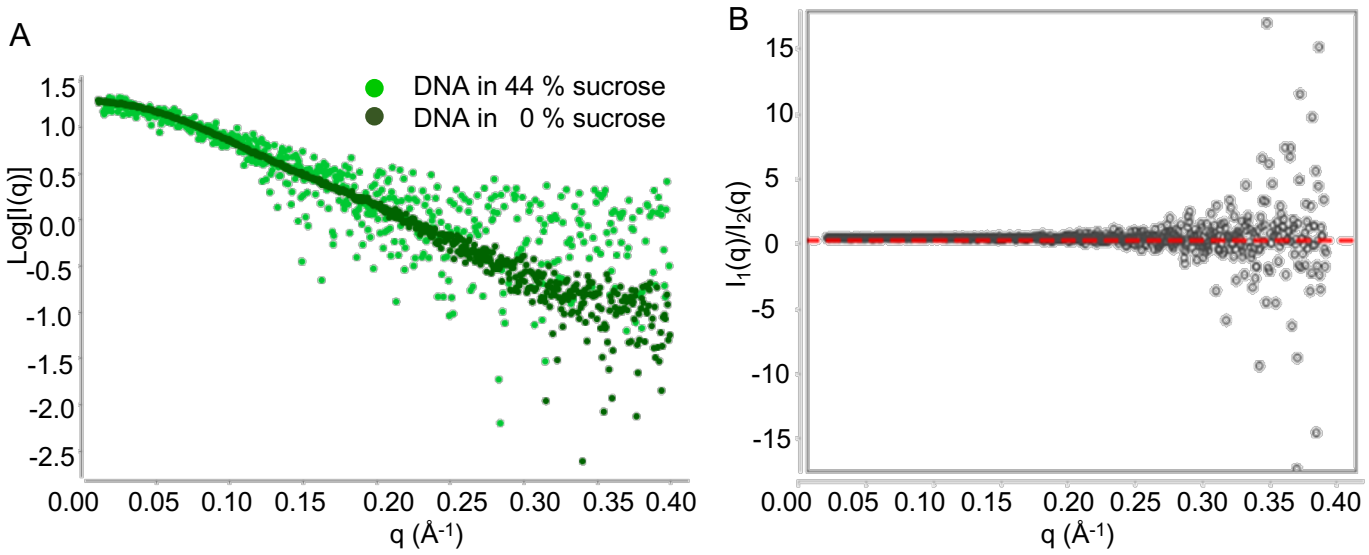
A
DNA in 44 % sucrose
DNA in 0 % sucrose
Log[I(q)]
1.5
1.0
0.5
0.0
-0.5
-1.0
-1.5
-2.0
-2.5
0.00 0.05 0.10 0.15 0.20 0.25 0.30 0.35 0.40
q (Å-1)
B
I1(q)/I2(q)
15
10
5
0
-5
-10
-15
0.00 0.05 0.10 0.15 0.20 0.25 0.30 0.35 0.40
q (Å-1)

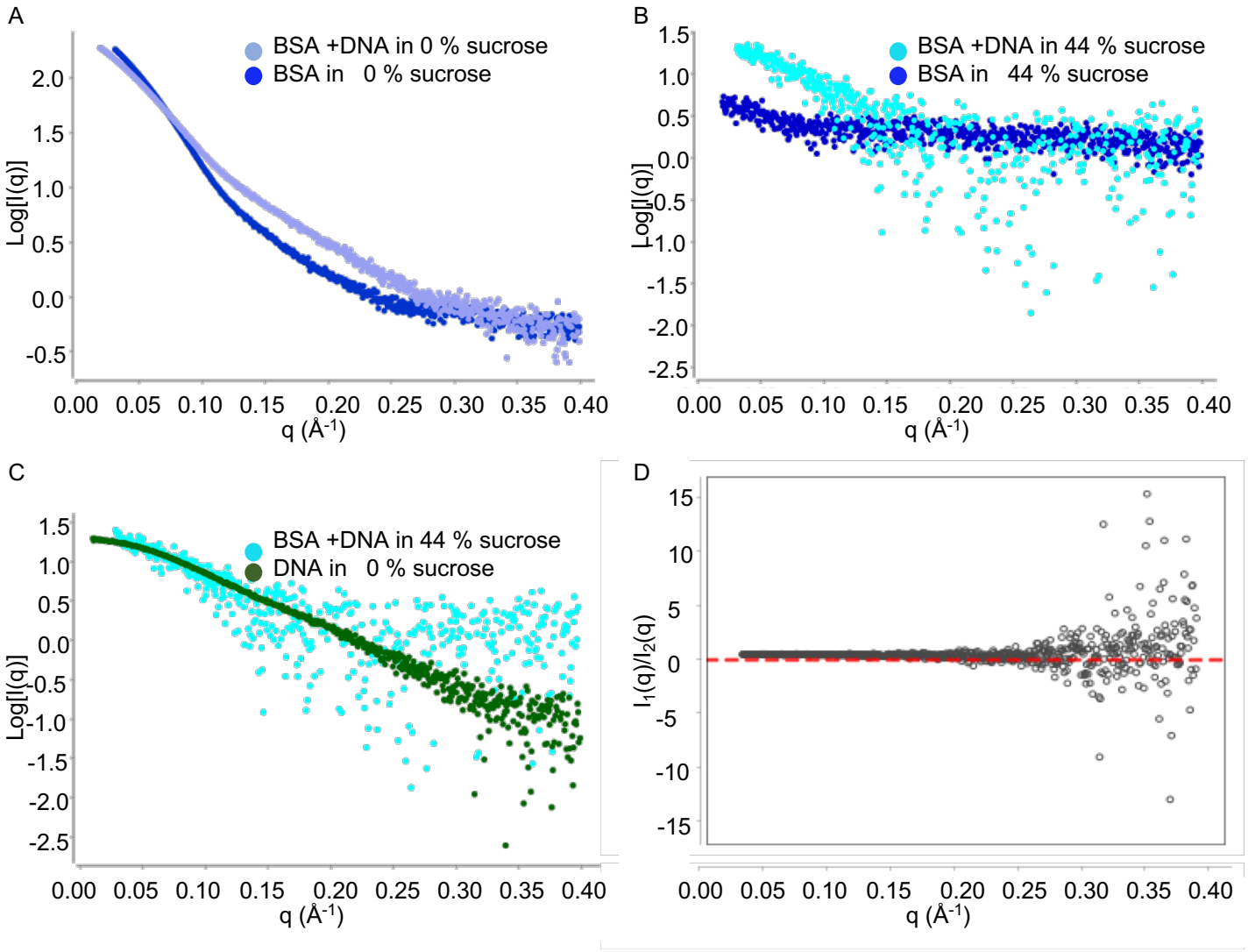
A
BSA +DNA in 0 % sucrose
BSA in 0 % sucrose
Log[I(q)]
q (Å-1)
B
BSA +DNA in 44 % sucrose
BSA in 44 % sucrose
Log[I(q)]
q (Å-1)
C
BSA +DNA in 44 % sucrose
DNA in 0 % sucrose
Log[I(q)]
q (Å-1)
D
I1(q)/I2(q)
q (Å-1)

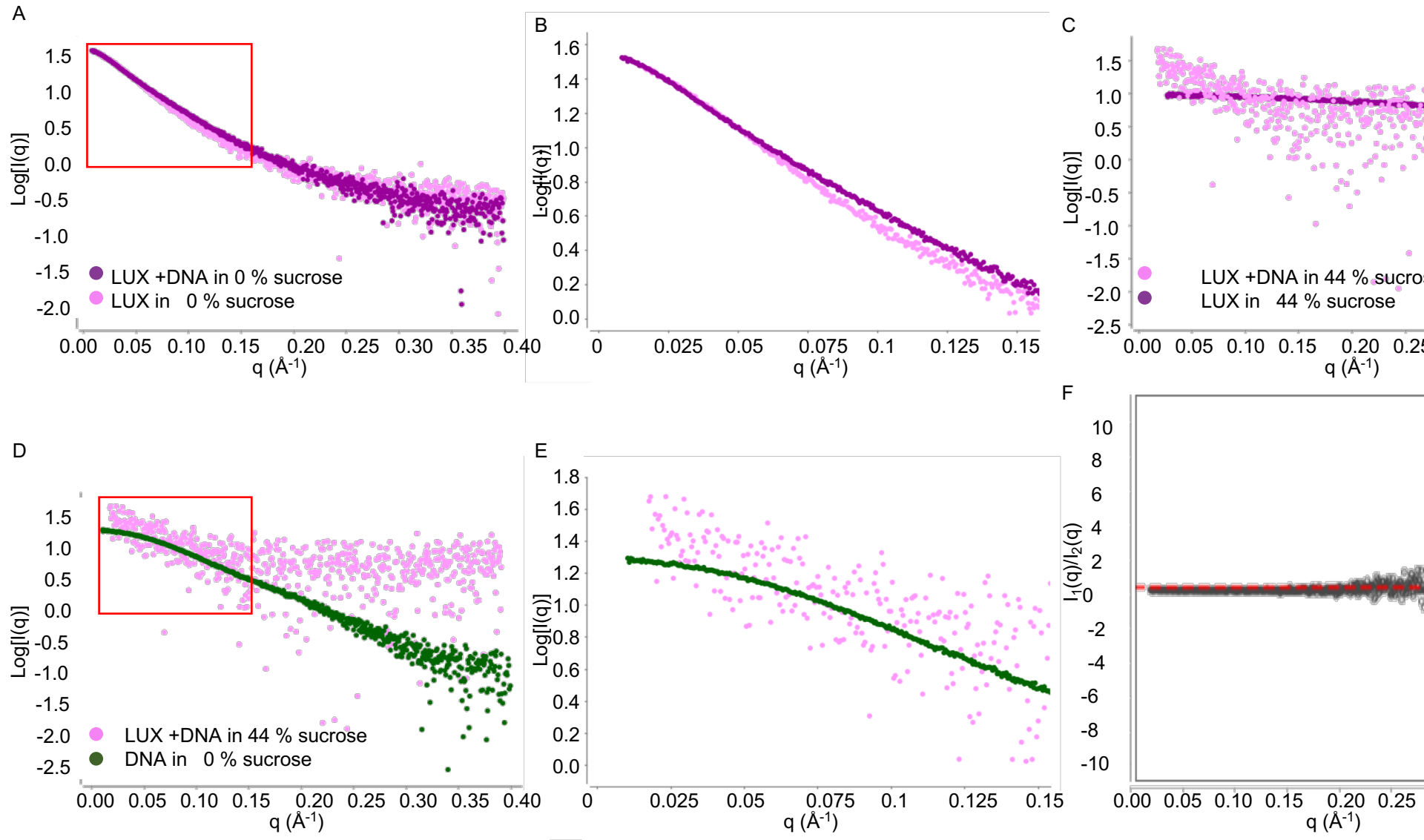
A
Log[I(q)]
q (Å-1)
LUX +DNA in 0 % sucrose
LUX in 0 % sucrose
B
Log[I(q)]
q (Å-1)
C
Log[I(q)]
q (Å-1)
LUX +DNA in 44 % sucros
LUX in 44 % sucrose
D
Log[I(q)]
q (Å-1)
LUX +DNA in 44 % sucrose
DNA in 0 % sucrose
E
Log[I(q)]
q (Å-1)
F
I1(q)/I2(q)
q (Å-1)